J. Fluid Mech. (1989), *vol.* 203, *pp.* 449–473
Printed in Great Britain

The stress tensor for simple shear flows of a granular material

By CHARLES S. CAMPBELL
University of Southern California, Department of Mechanical Engineering, Los Angeles, CA 90089-1453, USA

(Received 9 January 1987 and in revised form 21 October 1988)

The complete stress tensor has been measured using a computer simulation of an assemblage of rough, inelastic spheres in an imposed simple shear flow. Only five components of the stress tensor were found to be significantly different from zero. These represent the disperssive normal stresses τ_{xx}, τ_{yy} and τ_{zz} and the in-the-shear-plane shear stresses τ_{xy} and τ_{yx}; furthermore, the two off-diagonal stresses, τ_{xy} and τ_{yx}, were found to be equal so that the resultant stress tensor is symmetric. Two modes of microscopic momentum transport produce the final macroscopic stress tensor: the streaming or kinetic mode by which particles carry the momentum of their motion as they move through the bulk material, and the collisional mode by which momentum is transported by interparticle collisions. The contribution of each to the final result is examined separately. The friction coefficient, the ratio of shear to normal force, is shown to decrease at dense packings for both the collisional and streaming modes. Also observed were normal stress differences, both in and out of the shear plane, reflecting anisotropies in the granular temperature.

1. Introduction

Compared to most other branches of fluid mechanics, the flow of granular materials is still quite a mystery. In part, problems arise because a granular material is, of course, solid and only adopts fluid behaviour under special circumstances. When an appropriate state of stress is applied to a static granular material, it will yield along stress characteristics, much like an ideal plastic material. If the deformation is slow enough, the motion will continue in this fashion; i.e. the material will flow as large blocks, each consisting of many granules, moving relative to one another along thin slip lines. This is the 'quasi-static regime' of granular flow. However, if the deformation occurs rapidly enough, the impact between particles along the slip lines will be sufficient to dislodge the particles from their parent blocks of granules, continually enlarging the intervening slip region until the entire mass of material is moving as independent grains, each in relative motion with even their nearest neighbours. To the eye, individual particles will appear to move in a random manner about the average motion of the bulk material. This latter case is the 'rapid flow' or 'grain inertia' regime. Within this regime, any contact between particles is momentary, as the relative motion which drives the particles together will soon draw them apart. A complete description of the flow field must then include both the average velocity of the bulk material and some description of the individual random particle velocities.

This concept of particles moving individually in a random manner within the context of a bulk material moving as a mass under the influence of applied forces,

strongly evokes the image of the thermal motion of molecules in the kinetic theory picture of gases. The analogy is so strong that the mean-squared average of the random velocities has been dubbed the 'granular temperature' and there has recently been a great deal of success in adapting hard-sphere molecular models to rapid granular flows, by using the granular temperature as a replacement for the thermodynamic temperature. Indeed, the granular and thermodynamic temperatures share many of the same macroscopic effects: both generate pressures, both are related to the local density and pressure through an equation of state, both control the transport rates which result in the apparent viscosity and thermal conductivity of the material, and both conduct 'thermal energy' along their gradients. (See Campbell & Brennen 1985*b*.) In the parlance of granular materials, the pressures associated with the granular temperature are referred to as 'dispersive stresses' as they act to force the particle centres apart (i.e. disperse the particles). From a macroscopic point of view, the dispersive stresses keep the local solid concentration small enough to maintain the bulk material in a fluidized state. Unlike molecules, however, the interactions between particles are inelastic and thus, breaking the analogy with the thermodynamic temperature, the granular temperature cannot be self-sustaining. Instead, to maintain the granular temperature, energy must be continually pumped down into it, from the energy of the mean flow, by the mechanism of shear work (i.e. the work done by stresses against the velocity gradient). Thus there is a three-tiered energy flow path within rapid granular flows: (i) work performed on the granular system by stresses applied at boundaries and/or by a body force such a gravity which collectively drive the bulk motion of the material; (ii) shear work generates granular temperature wherever there are velocity gradients in the mean flow; (iii) collisions between particles dissipate the granular temperature into thermodynamic heat. Steady motion of a granular material implies that the energy remains nearly constant so that whatever work is performed by external forces on the granular systems must eventually be dissipated away as heat by interparticle collisions. Understanding this energy path, is key to an understanding of the mechanical behaviour of rapid granular flows.

Bagnold (1954) performed the earliest detailed investigation into rapid granular flow. He studied wax spheres suspended in a glycerine–water–alcohol mixture, and sheared in a Couette shear cell. The results showed that even at moderate concentrations and shear rates, the composite ceases to behave like a Newtonian fluid with a corrected viscosity and adopts the behaviour:

$$\tau_{ij} = \rho_{\mathrm{p}} R^2 f_{ij}(\nu) \left(\frac{\mathrm{d}u}{\mathrm{d}y}\right)^2, \tag{1.1}$$

where τ_{ij} is the stress tensor, ρ_{p} is the density of the solid material, f_{ij} is a tensor-valued function of the solid fraction ν, ($\nu = \rho_{\mathrm{bulk}}/\rho_{\mathrm{p}}$ is the fraction of a unit volume that is occupied by solid), R is the particle radius, and $\mathrm{d}u/\mathrm{d}y$ is the local velocity gradient. This rule has been confirmed for dry granular materials by Savage & Sayed (1984), Hanes (1983), Hanes & Inman (1985), and by the fluid free computer simulations of Campbell & Brennen (1985*a*), Campbell & Gong (1986), Walton & Braun (1986*a*, *b*), Hopkins (1985) and Hopkins & Shen (1987). In fact, as long as the only timescale in the problem arises from the velocity gradient $\mathrm{d}u/\mathrm{d}y$, this behaviour may be anticipated from a simple dimensional analysis. As such, it is not surprising that all theoretical analyses, starting with the heuristic arguments of Bagnold (1954) and continuing through the progressively more sophisticated work of McTigue

(1978), Kanatani (1979*a*, *b*, 1980), Ackermann & Shen (1979), Ogawa & Oshima (1977), Oshima (1978, 1980), and Haff (1983), predict exactly the same behaviour for simple shear flows. The most comprehensive studies along these lines, described in Savage & Jeffrey (1981), Jenkins & Savage (1983), Lun *et al.* (1984), Lun & Savage (1987), Jenkins & Richmond (1985*a*, *b*, 1986) and Nakagawa (1987), are derived from Enskog's dense-gas model (see Chapman & Cowling 1970). The essential differences between the predictions of all of the theories for simple shear flows lies in the nature of the tensor-valued catchall function $f_{ij}(\nu)$.

Equation (1.1) indicates that the apparent viscosity of a rapid granular flow varies linearly proportionally to the shear rate. This is particularly interesting as Campbell & Brennen (1985*a*) showed, in their simple shear flow simulations, that the granular temperature is almost uniformly distributed across the gap and varies as the square of the shear rate. In this light, (1.1) indicates that the apparent viscosity of a granular flow varies as the square root of the granular temperature, much as simple kinetic theory arguments dictate that the viscosity of a gas should vary as the square root of the thermodynamic temperature. This is particularly intriguing as a recent experimental study, Campbell & Wang (1986), indicates that the effective thermal conductivity of a granular material in air also varies directly proportional to the shear rate (and thus with the square root of the granular temperature), just as would be expected from the kinetic theory of gases. (This may not be the case for more complicated flows. Campbell & Brennen (1985*b*) show that this is not the case for flow down an inclined chute, where there are large gradients in the granular temperature, and give evidence of a 'conduction' of granular temperature much like the conduction of heat in a solid. Similar phenomena are predicted in many of the theoretical models mentioned above.)

Recently the techniques of molecular dynamics computer simulations have been adapted to the study of macroscopic particle flows. Based on well-defined models of particle interactions – surface friction, collisions, elastic deformations, etc. – a mechanical system of granules is set up on a computer. Body forces are applied or the boundaries of the system are set in motion to induce flow within the particle assembly. 'Experiments' are then performed on the system by taking statistical averages of the system properties. As the instantaneous positions and velocities of the particles are known (which collectively describe the entire state of the system), literally everything about the system can be found in this manner, including many things that probably can never be found by direct experiment. This type of investigation is especially valuable in granular flows where the large particle concentrations make laboratory measurements extremely difficult. The first work along these lines was due to Cundall (1974), but while the utility of his simulation was evident by the modelling of some rapid granular flows such as the emptying of a hopper, the only quantitative measurements were of extremely slow flows which involved only small deformations of a granular assembly. Campbell & Brennen (1985*a*, *b*) were the first to apply this type of simulation to rapid granular systems, studying the flow down an inclined chute and in a Couette shear cell. This last was extended to make detailed stress tensor measurements by Campbell & Gong (1986) and studies of the effects of system boundaries by Campbell & Gong (1987) and Campbell (1987). Two-dimensional stress tensor measurements were independently performed by Walton & Braun (1986*a*) using a slightly different simulation technique. The general type of simulation has also been used by Werner & Haff (1985, 1986) and Haff & Werner (1986). Recently Hopkins (1985) and Hopkins & Shen (1987) have adapted the Monte Carlo method to granular flows, which shows

remarkably good comparison with the more exact models described above. A review of the various simulation methods can be found in Campbell (1986*b*).

Until the smooth particle studies of Walton & Braun (1986*b*), all of the above simulation efforts were performed on two-dimensional flows of discs or cylinders. This eased the extensive computational demands and allowed some excellent movies to be produced, but somewhat complicated the interpretation of the results. In particular, the geometrical differences between the two- and three-dimensional cases led to different interpretations of the space-filling effects of the solid fraction. Furthermore, there could be no measurement of out-of-shear-plane normal forces such as those reported in Savage (1979). The purpose of the current investigation is to extend the studies of Campbell & Gong (1986) to make a detailed study of the granular stress tensor in a simple shear flow of rough spheres.

2. Computer simulation

Other than its three-dimensional nature, this simulation is not markedly different from those used previously by Campbell (1982), Campbell & Brennen (1985*a*, *b*) and Campbell & Gong (1986). Throughout the simulation, spherical particles (of mass m and radius R) are confined within a control volume such as that shown schematically in figure 1. All of the sides of the control volume are bounded by 'periodic' boundaries; as a particle passes through one periodic boundary it re-enters the other with exactly the same position and relative velocity with which it left. This type of boundary gets its name because it simulates a situation in which the control volume and its particles are periodically repeated, infinitely many times upstream and downstream of the central control volume. For these simulations, similar boundaries are also used to close the top and bottom. This set-up greatly enhances the computational efficiency of the simulation by limiting the number of particles to those initially placed in the control volume. It has the drawback that it is only applicable to flows with no gradients in the flow direction (i.e. steady, unidirectional flows).

The major difference between this simulation and that used by Campbell & Brennen (1985*a*, *b*) and Campbell & Gong (1986) is that there are no solid boundaries enclosing the control volume. In the previous simulations, the shear flow was driven by two solid walls, separated by a distance H in the y-direction, and set in relative motion in the x-direction with velocity U, to impose a shear rate U/H. (Here and in the following discussion, the x-direction will refer to the direction of mean motion. The boundaries of the system generate a mean field velocity gradient in the y-direction. The out-of-the-shear-plane coordinate will be referred to as the z-direction.) In these most recent simulations, shown schematically in figure 1, the solid walls are eliminated and the control volume is closed in the y-direction by periodic boundaries separated by a distance H. To similarly impose a shear rate U/H, the periodic images that bound the top and bottom of the control volume are set in motion with velocities $\frac{1}{2}U$ and $-\frac{1}{2}U$, respectively, in the x-direction. That is, when a particle exits the bottom of the central control volume, it re-enters the top with its x-direction velocity increased by U and a displaced x-coordinate that reflects the displacement of the origin of the moving periodic image. The opposite path is followed by particles that exit through the top of the control volume. This type of boundary is similar to that used by Walton & Braun (1986*a*, *b*) but can be attributed originally to Lees & Edwards (1972). The major benefit is that non-uniformities, such

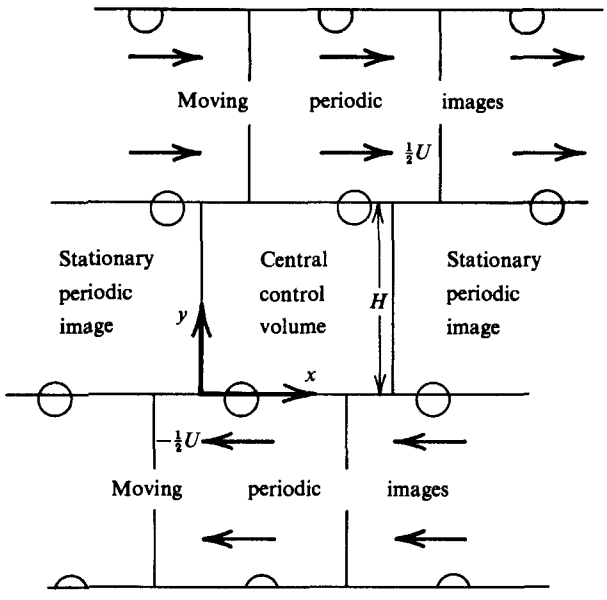

FIGURE 1. Central stationary control volume and its eight neighbouring periodic images. One particle and its periodic images are shown crossing the control volume boundaries.

as those revealed in Campbell (1987) and Campbell & Gong (1987), are not imposed on the system by solid boundaries.

Most of the current work was performed on control volumes of 240 particles which were originally arranged in a $6 \times 10 \times 4$ (referring ot the x-, y- and z-directions) cubical array. The sole exception were the simulations performed at the largest solid fractions which were started from an initial $6 \times 5 \times 4$ array. This was done to limit the freedom of motion of the particles by introducing some relatively short-range order into the system and thus to prevent 'bridges' (an effectively solid percolation of particles) which would transmit large stresses across the extent of the control volume. In actual Couette flow experiments such bridges form across the shear gap, producing large stress fluctuations such as those noted by Savage & Sayed (1984). But to break such a bridge, and allow the continuance of the flow, the walls of their apparatus had to be allowed to momentarily expand, as if vaulted on a pole of particles, causing a momentary decrease in the local density. Exactly the same behaviour could be seen in the wall-bounded simulations of Campbell & Brennen (1985*a*) and Campbell & Gong (1986) which were equipped with moveable walls in an almost exact reproduction of the Savage & Sayed (1984) apparatus. As the dimensions of the control volume used in the current studies are fixed, in order to maintain a uniform value of the instantaneous solid fraction, such bridges, if allowed to form, would never clear and thus had to be prevented.

The particles interact by colliding with one another. Each collision is assumed to occur instantaneously once the particle surfaces come into contact (this is essentially the hard-sphere approximation often used in the kinetic theory of gases) and the collision result is computed from a standard centre-of-mass collision solution. Because the particles rotate as well as translate, two conditions are required to close the system of equations: one for the relative particle velocities normal to and one for

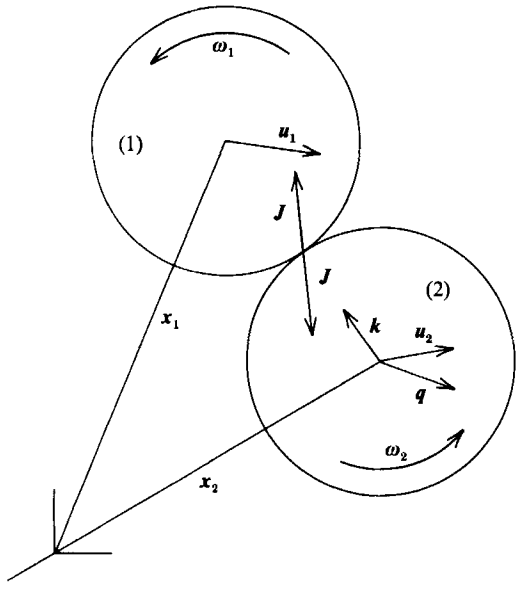

FIGURE 2. Diagram for the collision analysis.

the velocities tangential to the particle surfaces at contact. The normal velocity condition assumes that the particles are 'nearly elastic' in the sense that energy is dissipated as a result of the collision but the particles retain their spherical shape. This is realized in the simulation through a coefficient of restitution $\epsilon(\epsilon < 1)$, which is the ratio of the approach to recoil velocities, and is specified as an input parameter to the program. For the tangential condition, the particle surfaces are assumed to be fully rough in the sense that surface friction will always be large enough to stop any relative motion of the particle surfaces tangential to the point of contact. The impulse, $\boldsymbol{J}$, exerted by the collision is then (referring to figure 2)

$$\boldsymbol{J} = \tfrac{1}{2}m(1+\epsilon)(\boldsymbol{q}\cdot\boldsymbol{k})\boldsymbol{k} + \frac{m\beta}{2(1+\beta)}(\boldsymbol{q}-(\boldsymbol{q}\cdot\boldsymbol{k})\boldsymbol{k} + R(\boldsymbol{\omega}_1+\boldsymbol{\omega}_2)\times\boldsymbol{k}), \tag{2.1}$$

where m is the mass of the particle, $\boldsymbol{q} = \boldsymbol{u}_1 - \boldsymbol{u}_2$ is the relative velocity of the particles just before collision, $\boldsymbol{\omega}_1$ and $\boldsymbol{\omega}_2$ are the particle angular rotation rates, β is the ratio of the square of the particle radius of gyration to the square of the particle radius, and $\boldsymbol{k} = (\boldsymbol{x}_2 - \boldsymbol{x}_1)/\|\boldsymbol{x}_2 - \boldsymbol{x}_1\|$ is the unit vector pointing along the line connecting the particle centres at the instant of collisions. (Here, $\boldsymbol{x}_1$ and $\boldsymbol{x}_2$ are vectors pointing from the origin to the centres of particles 1 and 2 respectively.)

After the initial configuration and velocities of the particles and boundaries are chosen, the simulation is allowed to proceed as it will, with no outside intervention, until it converges to a steady state. (For these simulations, a converged state was assumed to occur when the total system kinetic energy achieves nearly constant values. However, like all small thermodynamic systems, the kinetic energy will fluctuate slightly with time, making the determination of convergence somewhat difficult.) Starting from the initial state, convergence was achieved after as little as 500 collisions per particle for most of these simulations.

3. Stress tensor measurements

As in common fluids, what are perceived as continuum stresses are a byproduct of the microscale mechanisms of momentum transfer within the material. For granular materials and hard-sphere models of gases, momentum is transferred in two modes. The 'streaming' or 'kinetic' mode describes the transport of momentum as a particle moves through the material carrying the momentum of its motion with it. The 'collisional' mode, as the name implies, describes the transport of momentum by interparticle collisions. Both mechanisms make important contributions to the stress tensor in a granular flow although, obviously, the streaming mode will dominate at low densities where collisions are infrequent and particles move long distances between collisions, while the collisional mode will dominate at high densities where collisions are frequent and particles cannot move far before colliding. The complete stress tensor is found by summing the contributions of both the streaming and collisional modes.

The streaming portion of the stress tensor, $\boldsymbol{\tau}_s^*$, is a byproduct of the random, almost thermal, motion of the granules. By arguments such as those presented in Chapman & Cowling (1970), the resulting contribution to the stress tensor is

$$\boldsymbol{\tau}_s^* = \rho_p \nu \begin{bmatrix} \langle u'^2 \rangle & \langle u'v' \rangle & \langle u'w' \rangle \\ \langle u'v' \rangle & \langle v'^2 \rangle & \langle v'w' \rangle \\ \langle u'w' \rangle & \langle v'w' \rangle & \langle w'^2 \rangle \end{bmatrix}, \tag{3.1}$$

where the primed quantities indicate the instantaneous deviation from the mean velocity. The symbol $\langle\ \rangle$ represents the average of the appropriate system properties, sampled at regular intervals, over a long period of system time – about 2500 collisions per particle. (For more details about the averaging process, the reader is referred to Campbell 1982.) Each term of the stress tensor is determined by the formula

$$\langle p'q' \rangle = \langle pq \rangle - \langle p \rangle \langle q \rangle \tag{3.2}$$

in exactly the same way as the Reynolds stresses in a turbulent fluid are computed from hot-wire traces. The primed quantities represent the random motion of the particles and it is therefore appropriate to define the granular temperature, T, as

$$T = \langle \boldsymbol{u}'^2 \rangle + \beta R^2 \langle \boldsymbol{\omega}'^2 \rangle. \tag{3.3}$$

As stated earlier, momentum is also transferred between particles when they collide. As the collisions are instantaneous, each results in an instantaneous momentum exchange equal to the collision impulse $\boldsymbol{J}$. From a transport point of view, the effect of a collision is the transport of $\boldsymbol{J}$-momentum a distance $2R$ in the direction $\boldsymbol{k}$. The effective momentum transport by a single collision across a surface separating the particles is $2R\boldsymbol{J}\boldsymbol{k}\cdot\boldsymbol{n}$, where $\boldsymbol{n}$ is the normal vector to the surface. That portion of the stress tensor, $\boldsymbol{\tau}_c^*$, that is due to interparticle collisions is thus given by:

$$\boldsymbol{\tau}_c^* = 2R[\boldsymbol{J}\boldsymbol{k}], \tag{3.4}$$

where $[\boldsymbol{J}\boldsymbol{k}]$ is found by summing the dyadic product $\boldsymbol{J}\boldsymbol{k}$ for every collision and, at the conclusion of sampling, dividing the result by the system volume and the length of the averaging period. (Physically the [ ] average should be interpreted as the $\langle\ \rangle$ average multiplied by the collision rate.)

As in Campbell & Gong (1986), the complete stress tensor is determined by summing the collisional and streaming contributions. The results are shown in

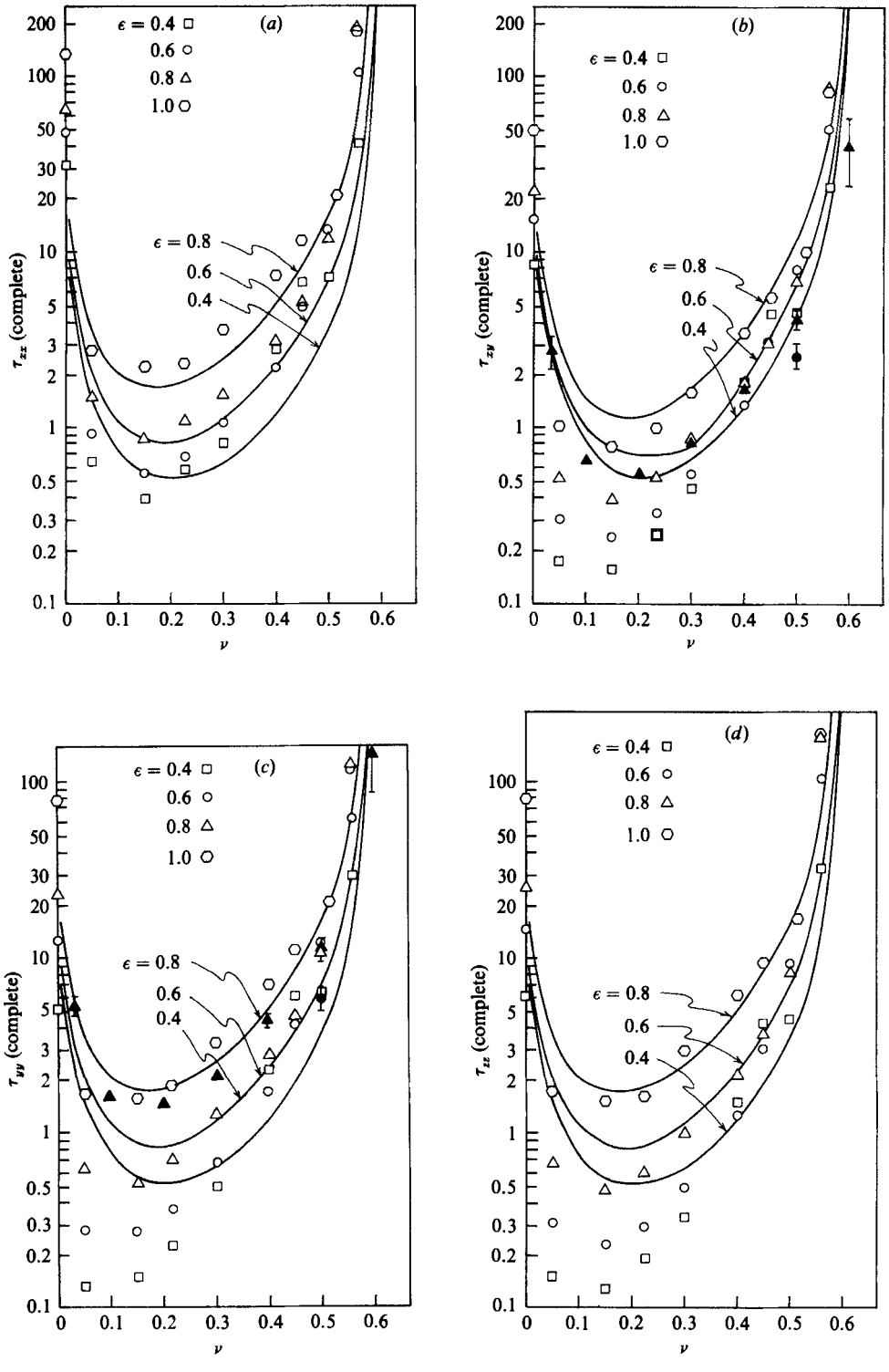

FIGURE 3. The complete dimensionless stress tensor as a function of the solid fraction ν: (*a*) τ_{xx}; (*b*) τ_{xy}; (*c*) τ_{yy}; (*d*) τ_{zz}. The lines are derived from Lun *et al.* (1984) and the solid symbols are from the smooth-particle simulations of Walton & Braun (1986*b*).

figure 3. The measured values of the τ_{xz}, τ_{zx}, τ_{yz} and τ_{zy} terms were several orders of magnitude smaller than the others indicating that, at least for simple shear flows, they are for all intents and purposes zero (exactly as predicted by all the theoretical studies) and are thus excluded from the reported data. The measured values for the off-diagonal stress tensor components τ_{xy} and τ_{xy} were found to be equal to within three significant digits and, as a consequence, no plots will be presented for the τ_{yx} component. This leaves only four components, τ_{xx}, τ_{xy}, τ_{yy} and τ_{zz}, to be reported. As for all that are to follow, these results are scaled as

$$\tau_{ij} = \frac{\tau_{ij}^* H^2}{\rho_p R^2 U^2}, \tag{3.5}$$

where τ_{ij}^* are the original unscaled results obtained from the simulation and U/H is the shear rate imposed by the moving periodic boundaries of the system. A simple dimensional analysis indicates that the resulting dimensionless stresses should be functions only of the particle coefficient of restitution ϵ and some dimensionless measure of the particle packing, here represented as the solid fraction ν. (For this flow geometry and boundary conditions, the scaled value, τ_{ij}, is interchangeable with f_{ij} in (1.1).)

Also plotted are the theoretical predictions of Lun *et al.* (1984). The comparison between the two sets of data is somewhat difficult because the Lun *et al.* data were derived for assemblies of smooth spheres while the data points come from fully rough particle simulations. Such a comparison is not completely irrelevant since the momentum transferred in a collision through surface friction is an order of magnitude smaller than that transmitted by the impact normal to the surfaces at the point of contact. These are included here because it is the most advanced theory available and, as yet, there is no theory that can include reasonable amounts of surface friction for dense mixtures of particle. (The problem has recently been solved for disks in the dilute limit by Nakagawa 1987.) Furthermore, the theoretical results compared remarkably well with the two-dimensional simulation of Campbell & Gong (1986) as long as an adjustment was made for the geometrical differences in the interpretation of the solid fraction. In fact, the theory compares much better with the two-dimensional than the three-dimensional results. This is a bit surprising since the theory was developed for three-dimensional flows of spheres rather than discs and in that context it appears that the agreement with the two-dimensional results was probably accidental. Following the suggestion of one of the authors of the Lun *et al.* paper (S. B. Savage 1984, personal communication), the particle pair correlation used in the calculations has been replaced with

$$g(\nu) = \left(1 - \frac{\nu}{\nu_m}\right)^{-2.5\nu_m}, \tag{3.6}$$

which had been found as a better fit to the data from molecular Monte Carlo simulations. Here ν_m is the maximum shearable solid fraction which was taken to be $\nu_m = 0.60$. No theoretical line is plotted for $\epsilon = 1.0$ as, with no particle surface friction, there would then be no energy dissipation mechanism within the Lun *et al.* system to damp the granular temperature; but granular temperature would still be generated by shear work so that, in such a case, its magnitude would continually increase and never reach steady conditions. Also, Lun *et al.* used only a first-order correction to a Maxwellian velocity distribution function in their analysis, and as such their results should only be applicable to flows that are not far from equilibrium,

i.e. small velocity gradients and small energy dissipation. The curves plotted for $\epsilon = 0.8$ may just barely fall inside their range of validity while the curves for $\epsilon = 0.4$ and $\epsilon = 0.6$ probably do not.

The other item that cannot be accounted for in the Lun *et al.* theory is the possible development of a shear-induced microstructure at large solid concentrations within the bulk material. Such a microstructure was observed in the two-dimensional simulations of Campbell & Brennen (1985*a*). They showed that, in order to maintain a shear flow at large density, the two-dimensional particles align themselves into layers oriented in the direction of mean flow: this organization allows almost unrestricted motion between the layers and thus permits a shear flow at concentrations that, without the layer formation, would probably exhibit solid behaviour. The layers affect the collisional stresses indirectly by inducing strong anisotropies in the collision angle distribution (i.e. the probability that a collision will occur at a given unit vector $\boldsymbol{k}$, connecting the particles centres). As the collisional stress tensor is formed by the average of the dyadic product $[\boldsymbol{Jk}]$, favoured values of $\boldsymbol{k}$ can strongly affect both the absolute and relative magnitude of the stress tensor components. (This is doubly true as, from (2.1), the collision impulse $\boldsymbol{J}$ itself depends on $\boldsymbol{k}$.) No observations of an equivalent microstructure development have been reported for assemblies of rigid spheres. However, molecular dynamics studies of Leonard–Jones molecules performed by Heyes (1986) indicate that shearing forces the molecules to align themselves into linear 'strings' of molecules pointing roughly in the direction of flow (corresponding to the x-direction in the current simulations). The strings organize themselves in a triangular packing in what here would be the (y, z)-plane. A shear motion can be maintained at high density within such a packing by relative motion between the strings in much the same way as a two-dimensional shear motion was maintained by relative motion between the layers. It seems reasonable to expect that a similar microstructure forms at high density in granular shear flows, especially as it appears to be the least restrictive organization that would kinematically permit a shear flow. One might guess, however, that owing to the additional degree of freedom, the three-dimensional microstructure is much less restrictive than its two-dimensional counterpart. At present, there is no theoretical model for the evolution of the microstructure and thus the microstructure effects could not be accounted for in the predictions of Lun *et al.* (1984).

The plots for τ_{xy} and τ_{yy} (figures 3*b* and 3*c*) also include data from the smooth-particle simulations of Walton & Braun (1986*b*). Unfortunately, most of their simulations were performed for larger coefficients of restitution and the only data that could be directly compared were for $\epsilon = 0.8$ and a single point at $\epsilon = 0.6$. The error bars on the points reflect the spread in their data with shear rate. The spread exists because Walton & Braun (1986*b*) use a 'soft-particle' model, in which the collision time is not instantaneous. (The rigid-particle model used here assumes that collisions occur instantaneously. A discussion of the various simulation methods can be found in Campbell 1986*b*.) Now the only timescale in the rigid-sphere model is the inverse shear rate, which makes equation (1.1) a dimensional certainty. The soft-particle model introduces the collision time as a new timescale into the problem and opens up the possibility that the ratio of collision time to the inverse shear rate may have an effect on the function $f_{ij}(\nu)$ in (1.1). It is interesting to note that the largest spread in the Walton & Braun data occurs at the largest density when the collision time becomes of the same order or longer than the time between collisions.

Similar to the results obtained from the two-dimensional simulation of Campbell &

Gong (1986), all of the τ_{ij} curves shown in figure 3, show a characteristic U-shape with asymptotes to infinity at $\nu = 0$ and at the shearable limit, $\nu \to \sim 0.6$. (The points shown at $\nu = 0$ were actually computed at a solid fraction of $\nu \approx 0.01$.) Exactly the same behaviour is observed in the Walton & Braun data and is predicted by Lun *et al.* (1984). As might be expected, there is very good agreement between the smooth-particle theory and the smooth-particle simulation, yet both predict significantly larger stress levels than are found in the rough-particle simulations. (Some of the apparent agreement between the rough- and smooth-particle data and the theory is artificial because the $e = 0.8$ curve corresponds closest to the $e = 1.0$ data points and the $e = 0.6$ curve corresponds best with the $e = 0.8$ data etc. It would be wrong to assume that the difference is due to the different simulation methods as comparisons in Campbell (1986*b*) show that both methods yield very similar results for rough particle simulations.) The large degree of disagreement between the rough- and smooth-particle data is somewhat surprising as wall friction appears to make only a small contribution to the stresses. (The two-dimensional simulations of Campbell & Gong 1986 show that the friction contributes about 10% of the total stress.) Thus there must be another mechanism that accounts for the large differences between the rough- and smooth-particle results. It may be reasonably speculated that the difference is largely due to the role that particle wall friction plays in dissipating away the granular temperature. Hence one would expect lower temperature levels with rough particles and with the lower temperatures, smaller collision rates (implying smaller collisional contributions to the stress tensor) and smaller streaming contributions to the stress tensor (as it is apparent from (3.1) that the streaming contribution is very closely related to the granular temperature).

The nature of the two asymptotes in figure 3 can be better understood by comparing the individual contributions of the collisional and streaming modes which are shown in figures 4 and 5 respectively. Each clearly accounts for one leg of the U shape of the complete stress tensor and thus the low-density asymptote can be attributed to the streaming contribution, and the high-density asymptote to the collisional contribution. The physical underpinning of the high-density asymptote is easy to understand. It occurs as the solid fraction approaches the shearable limit ($\nu \to \sim 0.6$) as beyond this limit, infinite stresses would be needed to initiate or maintain a shear flow. The explanation for the asymptote as $\nu \to 0$ is more elusive and is best understood by digressing for a moment to consider the energy flow in a granular material. Because energy is always dissipated in a collision, the energy associated with the granular temperature must be continually supplied by the shear work performed on the system, or else it would quickly dissipate away to nothing. Thus, the magnitude of the granular temperature depends on a tradeoff between the rate of shear work and the dissipation. The physical cause of the low-density asymptote may be understood by remembering that the dissipation rate is proportional to the collision rate while the stresses transmitted in the streaming mode are independent of the collision rate. Hence as $\nu \to 0$, the collision rate and, with it, the dissipation rate, go to zero. But, at the same time, there is still shear work performed as a product of the streaming stresses and the velocity gradient. Thus temperature is being produced at low density and, to maintain a steady flow, it must be dissipated by the few collisions that do occur. This implies that more energy must be dissipated per collision, which, as all the dissipation mechanisms are proportional to the impact velocity, implies large relative particle velocities and consequently a large granular temperature. Thus in the limit as $\nu \to 0$, the granular temperature

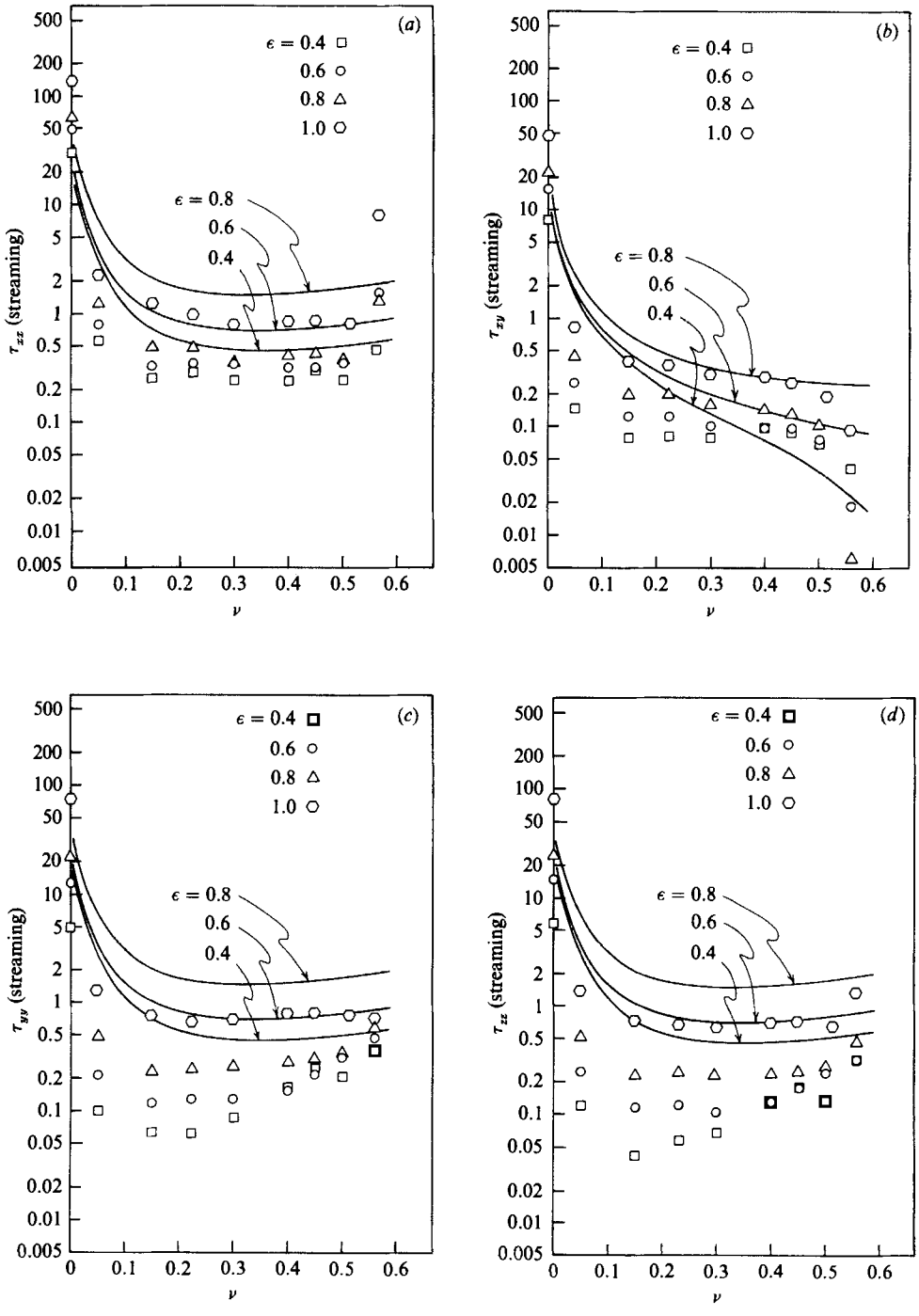

FIGURE 4. The streaming contribution to the stress tensor as a function of the solid fraction ν: (a) τ_{sxx}; (b) τ_{sxy}; (c) τ_{syy}; (d) τ_{szz}. The lines are derived from Lun *et al.* (1984).

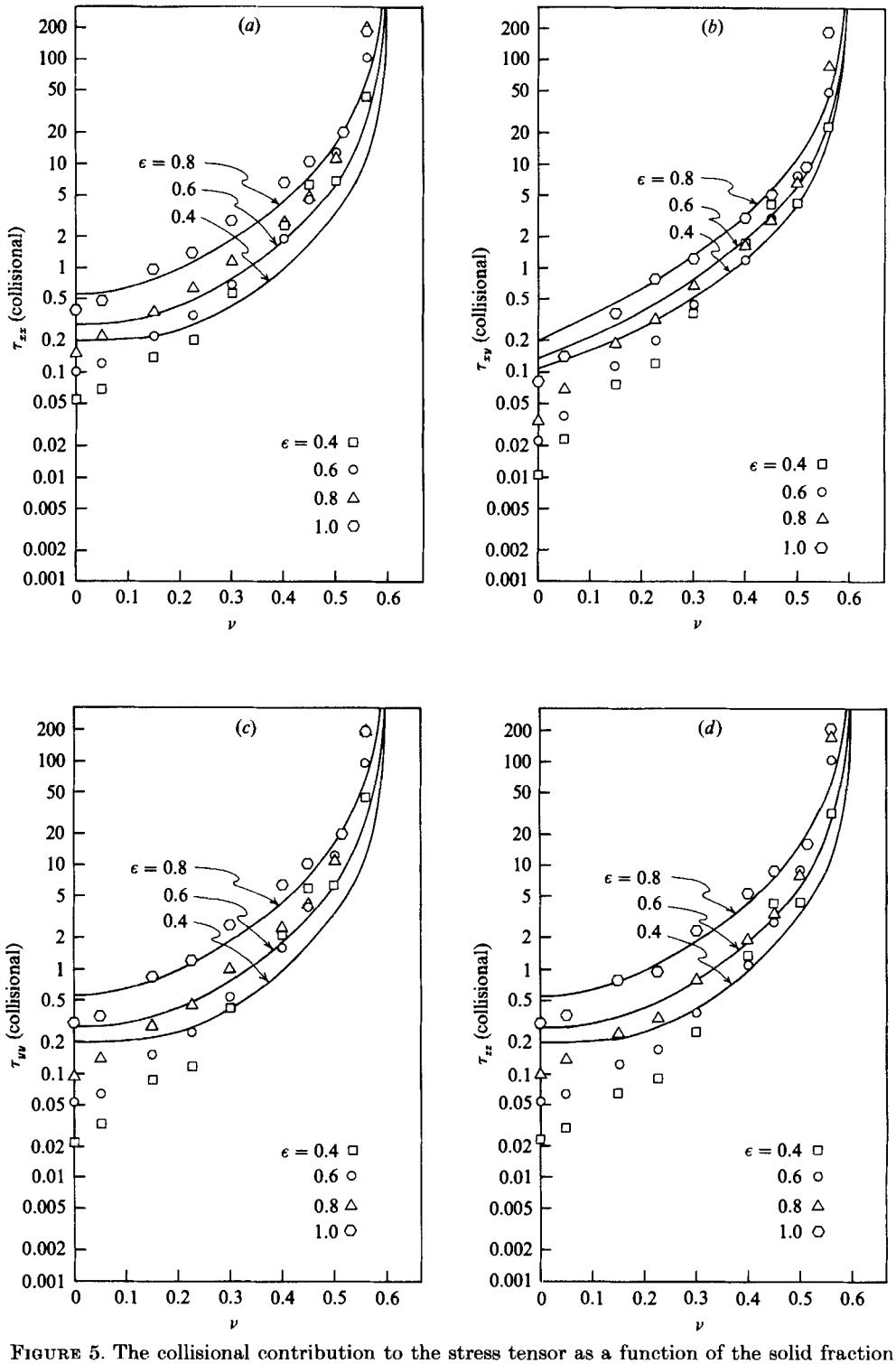

FIGURE 5. The collisional contribution to the stress tensor as a function of the solid fraction ν: (*a*) τ_{cxx}; (*b*) τ_{cxy}; (*c*) τ_{cyy}; (*d*) τ_{czz}. The lines are derived from Lun *et al.* (1984).

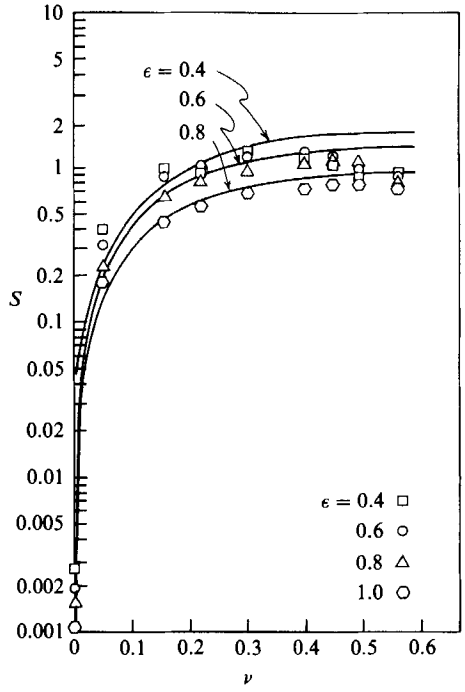

FIGURE 6. The dimensionless parameter S (equation (3.1)) as a function of the solid fraction ν. The lines are derived from Lun *et al.* (1984).

approaches infinity. The appearance of a low-density asymptote in figures 3 and 4 indicates that the $\langle u_i u_j \rangle$ correlations are going to infinity faster than ν is going to zero.

This process maybe better understood by considering the parameter

$$S = \frac{2RU}{HT^{\frac{1}{2}}}, \tag{3.7}$$

which is plotted in figure 6, along with the values predicted by Lun *et al.* (1984). Savage & Jeffrey (1981) first introduced this parameter (they denoted it R, but it is called S here to avoid confusion with the particle radius) and demonstrated its importance to transport processes in rapid granular systems. A physical interpretation of this parameter is that $1/S$ represents a kind of 'efficiency' by which the shear work (which is related to the velocity gradient U/H) generates the granular temperature, T. In figure 6, S is very small at small ν indicating that granular temperature is being generated very efficiently (presumably because the dissipation rate is going to zero along with the collision rate) while temperature is still being generated by the shear work performed against the streaming stresses. This is reflected in the stress asymptote as $\nu \to 0$. The parameter S increases dramatically for low values of the solid fraction but assumes a value very close to unity over much of the density range. Thus the dissipation of energy by inelastic collisions grows increasingly more important relative to the shear work as the density is increased and, consequently, the efficiency of the granular temperature generation is reduced; this continues until the two reach some sort of balance. (Note, it will be evident from figure 7 that S goes to unity at approximately the same point that the collisional

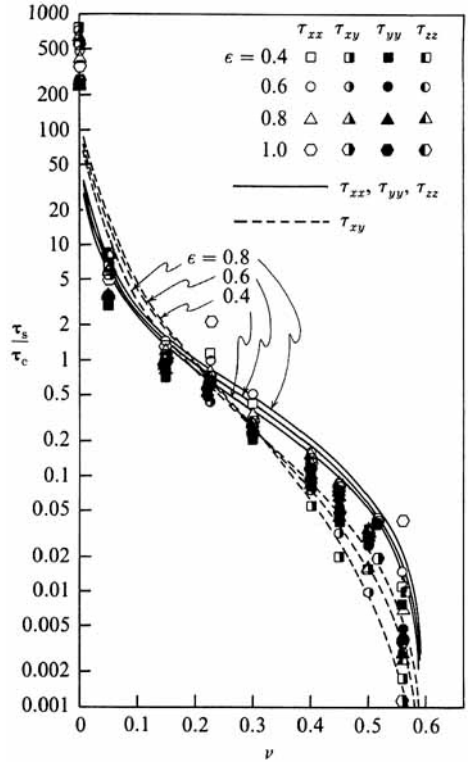

FIGURE 7. The ratio, τ_s/τ_c of streaming to collisional contributions to the stress tensor as a function of the solid fraction ν. The lines are derived from Lun *et al.* (1984).

stresses begin to dominate, i.e. just as the stresses begin to rise along the right leg of the U-shaped complete stress pattern shown in figure 3.)

Notice, in figure 3, that the points of minimum scaled stress are shifted far to the left of the minimum points predicted by Lun *et al.* (1984). At low densities, streaming stresses are dominant and the shifting of the minimum to the left in that region reflects a reduction in their importance. Furthermore, the shift becomes larger as the coefficient of restitution is reduced. This should be anticipated as the streaming stresses are closely related to the granular temperature and a smaller ϵ implies more energy dissipation and consequently a smaller granular temperature. When the streaming stresses are considered separately, as in figure 4, the reduction can be seen throughout the range of solid fractions. But this only becomes apparent for the complete stresses shown in figure 3 at low densities where the streaming stresses dominate. Notice that the minimum point for the $\epsilon = 0.8$ rough-particle simulation is shifted just slightly to the left of its smooth-particle counterpart, a fact that can similarly be attributed to the additional energy dissipated by the particle surface friction.

The relative importance of the collisional and streaming contributions, τ_s/τ_c, is shown in figure 7 along with the predictions of Lun *et al.* (1984). Note that the range of ν where the streaming stresses are important corresponds, as was anticipated, to the region where S is small. The Lun *et al.* study predicts that there should be minor variations in τ_s/τ_c with both density and stress tensor component. This variation is reflected somewhat in the simulation data but the scatter of the data is

much larger than any variation predicted by the theory. However, these results do show that the streaming and collisional contributions to the stress tensor have about the same magnitude at around $\nu = 0.15$, and that the streaming contribution becomes negligible ($\tau_s \approx 0.1\tau_c$) at about $\nu \approx 0.4$. The streaming stress tensor thus seems to be significantly less important in these three-dimensional simulations than for the two-dimensional flows examined by Campbell & Gong (1984). As it stands, it seems possible to ignore the streaming contributions to the stress tensor (as was popular in most of the early theoretical work) for much of the densities common in granular flows, as long as one keeps in mind that it may still be very important in some regions such as the low-density region observed near the chute bottoms by Campbell & Brennen (1985*b*).

By considering the nature of the collision impulse in equation (2.1), it should be surprising that the stress tensor ends up being symmetric. This is because the component of the impulse which is conveyed through friction between the particle surfaces, $\boldsymbol{J}'$,

$$\boldsymbol{J}' = \frac{m\beta}{2(1+\beta)}(\boldsymbol{q} - (\boldsymbol{q}\cdot\boldsymbol{k})\,\boldsymbol{k} + R(\boldsymbol{\omega}_1 + \boldsymbol{\omega}_2)\times\boldsymbol{k}), \tag{3.8}$$

is perpendicular to $\boldsymbol{k}$ and thus makes asymmetrical contributions to the collisional stress tensor when formed, as in (3.4), into dyadic products with the unit vector $\boldsymbol{k}$. However, $\boldsymbol{J}'$ is composed of two parts, that due to the relative motion of the particle centres tangential to the point of contact between the particles, $(\boldsymbol{q} - (\boldsymbol{q}\cdot\boldsymbol{k})\,\boldsymbol{k})$, (which in an averaged sense is related to the velocity gradient U/H) and that due to the particle rotation $(R(\boldsymbol{\omega}_1 + \boldsymbol{\omega}_2)\times\boldsymbol{k})$ (which will be related to the mean rotation rate, $\langle\boldsymbol{\omega}\rangle$, of the particles). Now, asymmetric stress are possible in a granular flow and may be interpreted as torques on the particles. The macroscopic manifestation of the torques will be either angular acceleration of the particles or spatial gradients in the mean rotation rates; however, as in steady flow there can be no time change in the mean rotation rate of the particles and, as the control volume configuration was chosen to prohibit any spatial gradients, the stress tensor must be symmetric. Campbell & Gong (1986) have shown in their two-dimensional simulation that, considered separately, the two contributions to $\boldsymbol{J}'$ do indeed make asymmetrical contributions to the stress tensor but, when considered together, the asymmetries cancel out. The granular flow accomplishes this naturally by fixing the mean rotation rate $\langle\boldsymbol{\omega}\rangle$ relative to the velocity gradient U/H. They showed that over most of the density range, $\langle\boldsymbol{\omega}\rangle\, H/U \approx -\frac{1}{2}$, but it decreases sharply as the shearable limit is approached. (Campbell 1986*a* has shown that the drop observed in the two-dimensional simulations is due to the microstructure development within the material.) The ratio $-\langle\boldsymbol{\omega}\rangle\, H/U$ is plotted in figure 8 as a function of the solid fraction ν. Over the entire range, $\langle\boldsymbol{\omega}\rangle$ has a value of about $-\frac{1}{2}H/U$ and is oriented perpendicular to the shear plane. This is more or less the same behaviour experienced by a particle in a fluid shear flow. The lack of the precipitous drop observed by Campbell & Gong (1986) at the larger solid fractions is one indication that the microstructure development is not as restrictive in three-dimensional flows of spheres as it is in two-dimensional disc flows.

As a side note, Campbell & Gong (1987) and Campbell (1987) have shown that asymmetric stresses may be found near boundaries as the boundary can itself impose a rotational state in the particles that collide with it that would be different from what the particle would naturally assume in a uniform shear flow. In that case, the torques induced in particles by the asymmetric stresses are balanced in steady flow by gradients in the corresponding couple stress tensor.

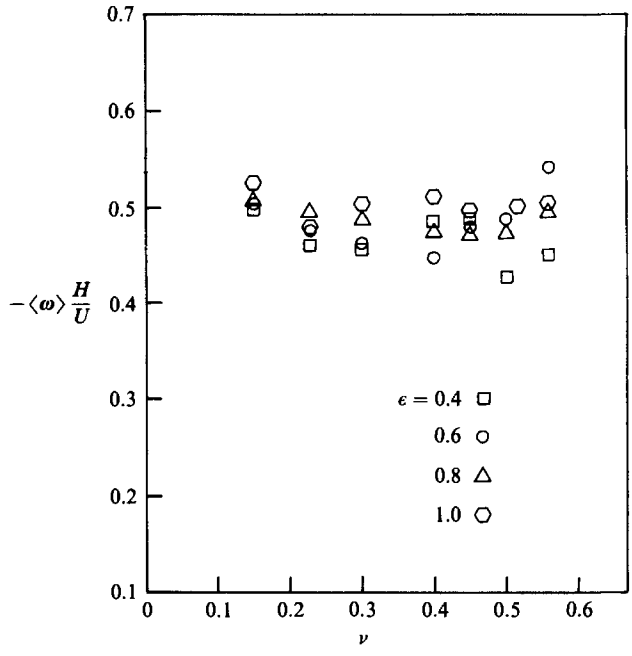

FIGURE 8. The scaled average rotation rate, $-\langle\omega\rangle H/U$, as a function of the solid fraction ν.

4. Friction coefficient and normal stress differences

Many important phenomenological features of a flow depend not so much on the stresses themselves but on the ratios between various components of the stress tensor. For example, the friction coefficient τ_{xy}/τ_{yy} represents the resistance applied by the shearing material relative to an applied normal stress and the differences between the normal stresses, reflected in the ratios τ_{xx}/τ_{yy} and τ_{yy}/τ_{zz}, will determine the degree to which the flow is subject to non-Newtonian normal stress difference effects.

Figure 9 shows the friction coefficient τ_{xy}/τ_{yy} plotted as a function of the solid fraction ν. The dominant feature is that the friction coefficient generally decreases with solid fraction. The smaller the coefficient of restitution the larger the absolute magnitude of the friction coefficient and the more severe the dropoff. In fact, τ_{xy}/τ_{yy} decreases monotonically only for $\nu = 0.4$, while for the larger coefficients of restitution, there are increasingly longer regions of solid fraction where the friction coefficient is effectively constant. (For $\nu = 1.0$, τ_{xy}/τ_{yy} is essentially constant for $\nu > 0.15$.) This drop in τ_{xy}/τ_{yy} was also observed in the shear-cell experiments of Savage & Sayed (1984). It is interesting to note that exactly the opposite effect is found in tests to determine the yield strength of soils; in these, an initially static sample is subjected to a shear force until it just begins to flow and the friction coefficient is determined as the ratio of shear to normal forces at the point of yield. Thus, the behaviour observed in these simulation results must reflect aspects of fully developed granular flows that are not present at the initiation of flow. As before the predictions of Lun *et al.* (1984) are also plotted. Campbell & Gong (1986) found a slightly better comparison between their data and a hybrid theory formed from a combination of the smooth-particle streaming stress tensor of Lun *et al.* (1984) and the collisional stress tensor from the rough-particle analysis of Lun & Savage (1987)

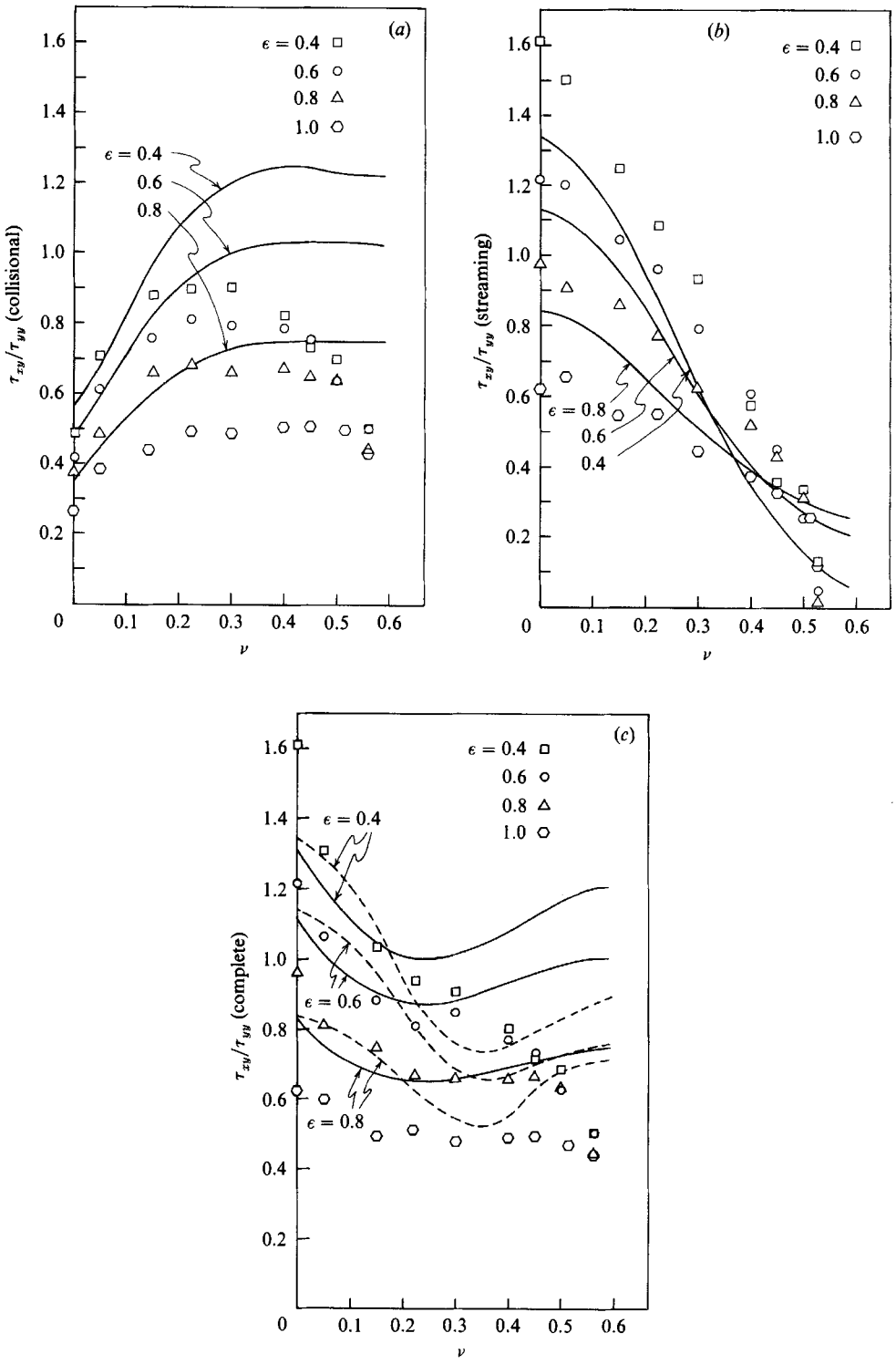

FIGURE 9. The friction coefficient τ_{xy}/τ_{yy} as a function of the solid fraction ν. (*a*) Collisional contribution, (*b*) streaming contribution, and (*c*) complete stresses. The lines are derived from Lun *et al.* (1984), and the dashed lines in (*c*) from Lun & Savage (1987) (hybrid).

(which neglected any streaming stresses and thus, by itself, compares poorly with the simulation data); this is plotted in figure 9(*c*) and, once again, the altered theory agrees better with the simulation results. In either case, the theories predict that τ_{xy}/τ_{yy} will decrease for small values of ν but will then increase towards the shearable limit.

To improve the physical understanding, the results are divided up to show the individual contributions of the collisional and streaming stress tensors. The streaming contribution to τ_{xy}/τ_{yy} is a decreasing function of ν and contributes most to the dramatic decline in the friction coefficient. Exactly the same trend in the streaming stresses is predicted by Lun *et al.* (1984). At the same time, the collisional contribution to the friction coefficient actually increases for small values of the solid fraction and only decreases as the shearable limit is approached. This latter decrease is not anticipated in the Lun *et al.* (1984) calculations, which predict that the friction coefficient should rise as the shearable limit is approached. Campbell (1986*a*) has shown that for two-dimensional flows the decrease in the collisional contribution to τ_{xy}/τ_{yy}, near the shearable limit, can be explained by the formation of the internal microstructure observed by Campbell & Brennen (1985*a*). Remember that the microstructure induces preferred choices of the collision vector $\boldsymbol{k}$ which will strongly affect the absolute and relative magnitudes of the components of the collisional stress tensor $\boldsymbol{\tau}_c = [\boldsymbol{Jk}]$. In two-dimensions the layer formation restricts a particle to collide with particles in its own layers and those in its two nearest neighbouring layers. Now, the particles from neighbouring layers restrict a particle's motion to a narrow band about the centreplane of the layer. Thus the collisions between particles within the same layer are restricted to a narrow range of angles about the midplane of the layer and the collisions with particles from neighbouring layers are restricted to a similarly narrow range of angles but are roughly perpendicular to those that occur between particles within the same layer. The similarity between the current results and their two-dimensional counterparts indicates that the behaviour of the collisional friction coefficient can be accounted for by an equivalent three-dimensional microstructure development such as the organization of particles into 'strings' as observed by Heyes (1986). Such a microstructure would affect on the three-dimensional collision angles in much the same way as the layered microstructure does in two dimensions. That is, collisions between particles within the same string occur about the poles of a particle while collisions between a particle and those in neighbouring strings would be more or less evenly distributed about the equator. This could explain the reduction in the collisional friction coefficient as the density is increased (and thus the microstructure becomes increasingly more confining). However, no clear connection can be made between the microstructure and the reduction in the streaming friction coefficient. As mentioned previously, the microstructure development could not be accounted for the Lun *et al.* theory, which explains why their predictions do not fall near the shearable limit.

Figures 10 and 11 show the variation of the normal stress ratios τ_{xx}/τ_{yy} and τ_{yy}/τ_{zz} as functions of the solid fraction ν. No theoretical lines are plotted because Lun *et al.* (1984) predict that there should be no normal stress differences. However, an earlier, though less complete, paper in that series, Savage & Jeffrey (1981), does predict that at large values of the parameter S, τ_{zz} is smaller than τ_{xx} and τ_{yy} (the latter two of which they predict to be equal). The data show that none of the normal stresses are equal and that for all values of ν, τ_{xx} is by far the largest, taking up to six times the value of the smallest, τ_{zz}.

Figure 10 shows a plot of the ratio τ_{xx}/τ_{yy} as a function of the solid fraction ν.

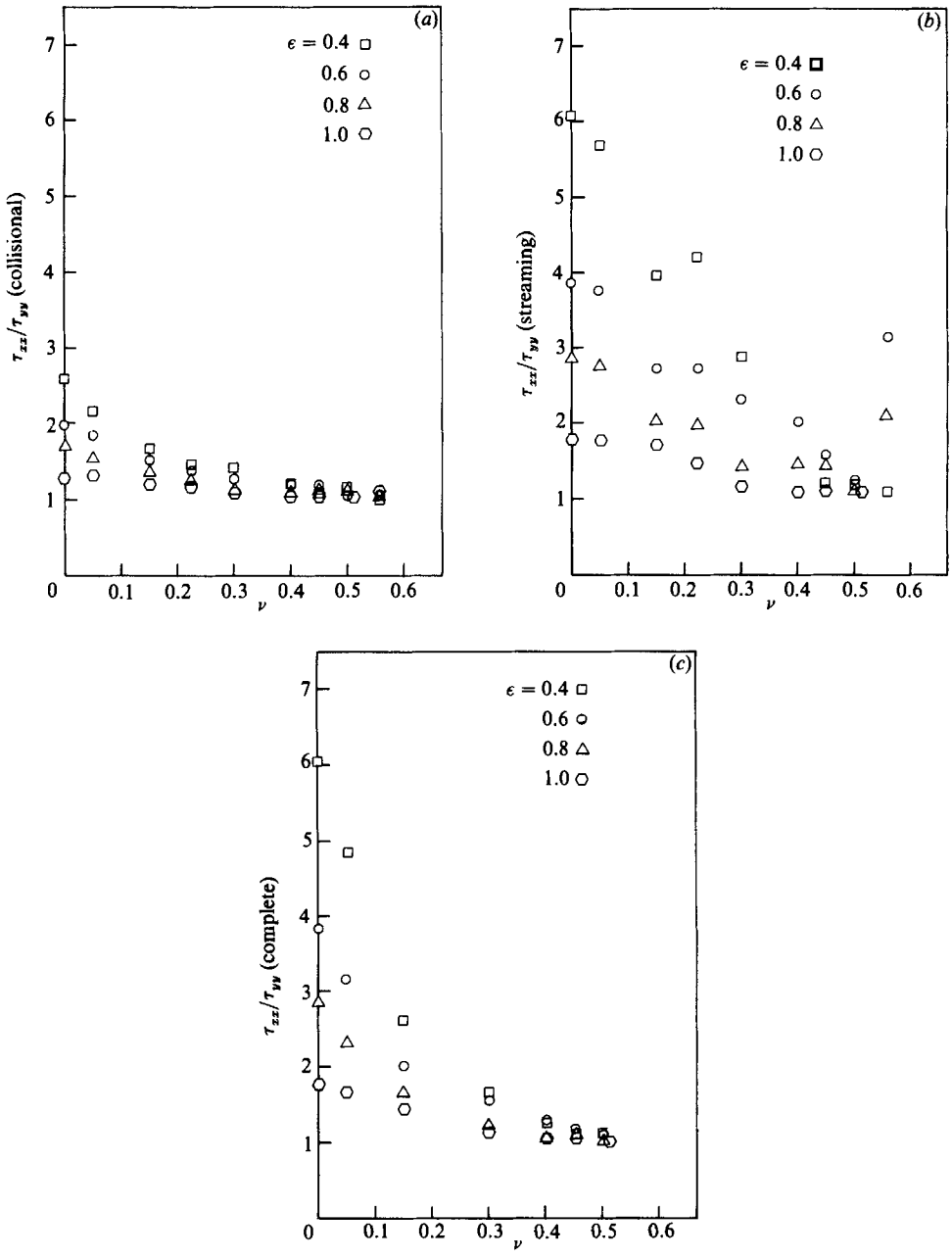

FIGURE 10. The ratio of in the shear plane normal stresses τ_{xx}/τ_{yy} as a function of the solid fraction ν. (*a*) Collisional contribution, (*b*) streaming contribution, and (*c*) complete stresses.

The ratio is observed to decrease monotonically towards an asymptotic limit slightly larger than 1 for all values of the coefficient of restitution ϵ. Furthermore, the smaller the ϵ, the more precipitous the fall of the ratio with ν. Like the friction coefficient most of the decrease occurs in the streaming contribution, although here the drop is mirrored in the collisional contribution. This may be better understood if the reader notes from (3.1) that the streaming component of τ_{xx}/τ_{yy} is just $\langle u'^2\rangle/\langle v'^2\rangle$, the ratio

of the temperature components in the x- and y-directions. Figure 10 (b) then indicates that, especially at low densities, the temperature in the x-direction is always greater than that in the y-direction. This, in turn, may be understood by examining the two mechanisms of temperature generation. By the first, or mode (i), temperature is generated as a byproduct of interparticle collisions; that is, even if the two colliding particles initially move with exactly the mean velocity appropriate to their position, the velocities of the particles after collision will have components that appear to be randomly distributed about the mean velocity. Macroscopically, this appears as granular temperature. The second, or mode (ii) temperature generation mechanism comes about from the granular–temperature-induced convection of a particle along the velocity gradients; i.e. that as a particle moves by virtue of its random motion along the gradients of mean velocity it will acquire an apparent random velocity, roughly equal to the difference in mean velocity between the particle's last collision and its present location. This latter mode of temperature generation will, of course, be largest for disperse flows where the particles move long distances between collision. Note that only x-direction temperature will be generated in mode (ii), as the simulation only has gradients of x-direction velocity. Thus, the mode (ii) temperature generation can explain why the temperature components in the x-direction are larger than those in the other directions and why the effect is largest at the smallest concentrations. Furthermore, the smaller the coefficient of restitution ϵ, the more energy that is dissipated in a collision and hence the smaller the magnitude of the random velocity produced in a collision by mode (i). Thus, the smaller the value of ϵ, the larger the relative importance of mode (ii) compared to mode (i) temperature generation and the larger the x-direction temperature, which is generated by both modes (i) and (ii), will be relative to the y- or z-direction temperatures (which can only be generated by mode (i)). Clearly, some process of this type is at work in figure 10. The temperature anisotropy would also cause collisions between particles to have a significantly larger x-direction, rather than y- or z-direction, impulse which can account for the minor variations in the collisional contribution to τ_{xx}/τ_{yy}. Finally, the streaming contribution to the friction coefficient, shown in figure 9 (b) may also be related to the temperature anisotropy as the drop in τ_{xy}/τ_{yy} with increasing solid fraction mirrors that in τ_{xx}/τ_{yy}; this would make sense as the temperature anisotropy implies a generally greater transport of x-direction relative to y-direction momentum. Note that figure 10 does not show the sudden rise as the shearable limit is approached that was apparent in the two-dimensional simulation of Campbell & Gong (1986) and explained by Campbell (1986a) as a byproduct of the layered microstructure development. This is another indication that whatever form the microstructure takes in three-dimensions is much less restrictive than its two-dimensional counterpart.

Figure 11 shows the other normal stress ratio τ_{yy}/τ_{zz} plotted again as a function of the solid fraction ν. The ratio starts at a value close to unity and rises; all the curves appear to flatten out towards the centre of the solid fraction range only, for all data except $\epsilon = 0.4$, to drop off again as the shearable limit is approached. This behaviour is reflected in both the streaming and collisional parts. The latter indicates that the y-direction temperature generation is favoured over the z-direction for much of the solid fraction range. However, no clear explanation of this observation is readily available to the author. (No plot is provided for τ_{xx}/τ_{zz} although, from comparison of figures 10 and 11, it can be seen that such a plot would show monotonically decreasing lines, slightly more precipitous than those in figure 10.)

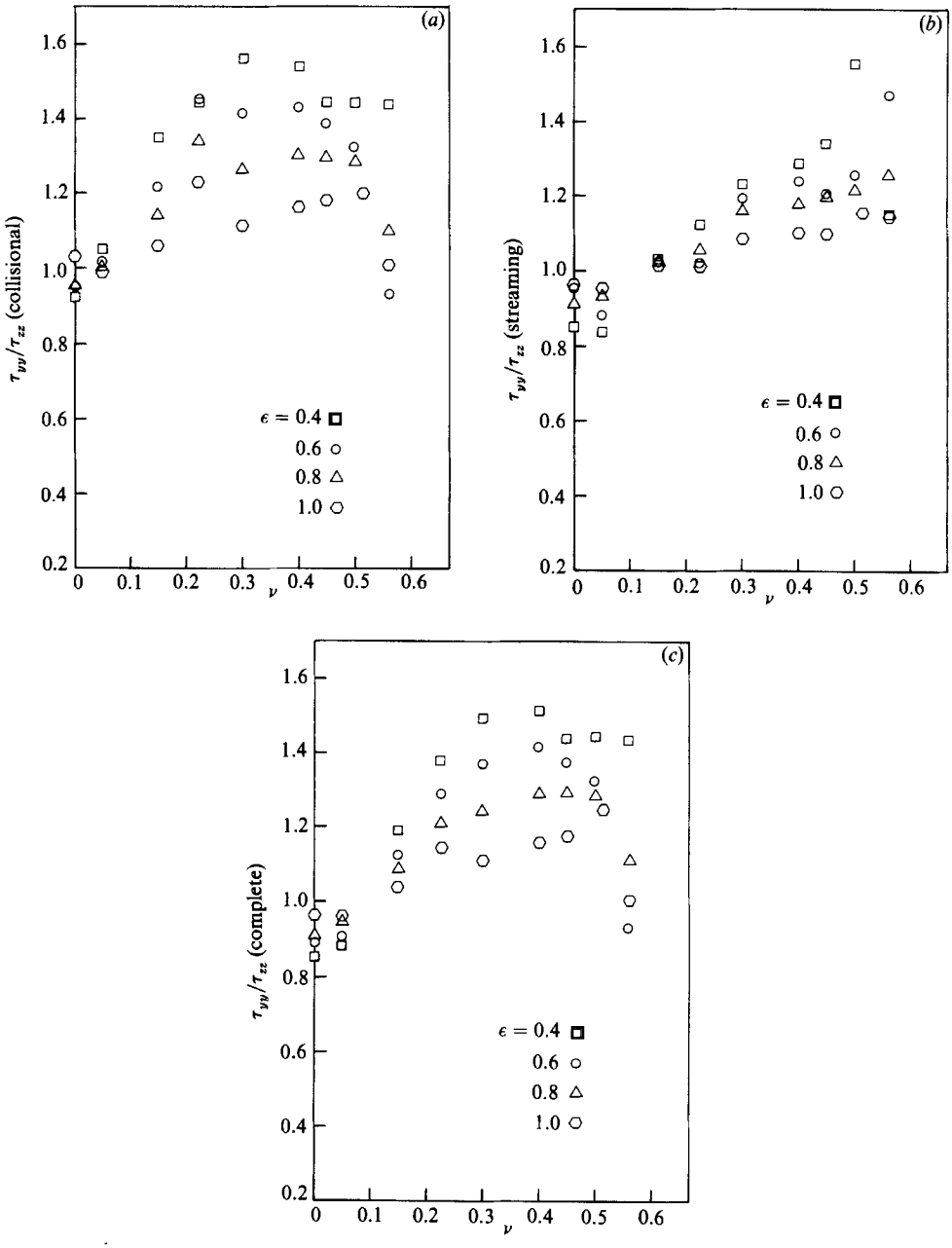

FIGURE 11. The ratio of normal stresses τ_{yy}/τ_{zz} as a function of the solid fraction ν. (*a*) Collisional contribution, (*b*) streaming contribution, and (*c*) complete stresses.

5. Conclusions

This paper has presented the results of a detailed study of the stress tensor that is generated in an imposed simple shear flow of inelastic rough spheres. The study was performed using a computer simulation which allows access to all the details of the flow. The stress tensor was found to be symmetric under all the conditions studied. Also, only four of the nine components, τ_{xx}, τ_{xy}, τ_{yy} and τ_{zz}, were reported

as the other components were found to be of insignificant magnitude. The complete stress tensor is a result of two microscopic mechanisms of momentum transport: (i) momentum transport by interparticle collision and (ii) the streaming mode whereby momentum is transported by the particles as they move along their random paths through the system, carrying their momentum with them. Naturally, the collisional mode dominates at dense particle packings where collisions are frequent and the streaming mode dominates for disperse packings where the particles move long distances between collisions.

The curves for all the components of the complete stress tensor have a characteristic U shape when plotted against solid fraction, each leg of the U representing an asymptote towards infinity, both as $\nu \to 0$ and as ν approached the maximum shearable concentration; the small-ν asymptote can be attributed to the streaming modes and the large-ν asymptote can be attributed collisional modes of momentum transport. The relative importance across the density range of the two modes was also examined and the results show the streaming stresses to be much less important for three-dimensional flows than for their two-dimensional counterparts. Even though the nature of the collision impulse admitted the possibility of asymmetric contributions within the collisional portion of the stress tensor, the measured stress tensors were nevertheless symmetric; as in the two-dimensional case, this is accomplished naturally in a granular shear flow by fixing the average rotation rate for the particles to a value of about half of the mean shear rate. Unlike the two-dimensional case, no precipitous drop was observed in the ratio $-\langle\omega\rangle H/U$ at high densities, which is an indication that the high-density microstructure that develops in a three-dimensional shear flow is significantly less restrictive than in the two-dimensional case. As was observed in numerous experiments and in the two-dimensional simulations, the friction coefficient τ_{xy}/τ_{yy} was found to be a decreasing function of the solid fraction ν. This observation was shown to arise in both the collisional and streaming contribution to the stress tensor. A similar observation can be made in the normal stress ratio τ_{xx}/τ_{yy} which was observed to be significantly different from unity over much of the parameter range. However, the three-dimensional results do not exhibit the sharp rise near the shearable limit that was apparent in the two-dimensional simulations. (This is an additional indication that the microstructural development in the three-dimensional simulations is much less restrictive than in two-dimensions.) This observation can be understood as a change in the relative importance of the two types of granular temperature generation. Conversely, the other normal stress ratio τ_{yy}/τ_{zz} was found to be a generally increasing function of the solid fraction, an observation for which there appear to be no immediate physical explanation.

The author would like to thank Ahn Trahn, Ailing Gong, Yi Zhang, David Wang and Doyle Howland for their assistance in preparing the figures. This work was performed under National Science Foundation grant number MEA-8352513 and additional funding provided by IBM, TRW and the Ralph Parsons Foundation. Special thanks to Drs George Lea, Stephan Traugott and Richard Miksad.

REFERENCES

Ackermann, N. L. & Shen, H. 1979 Stresses in rapidly sheared fluid–solid mixtures. *J. Engng Mech. Div. ASCE* **108**, 95–113.

Bagnold, R. A. 1954 Experiments on a gravity-free dispersion of large solid particles in a Newtonian fluid under shear. *Proc. R. Soc. Lond.* A **225**, 49–63.

CAMPBELL, C. S. 1982 Shear flows of granular materials. Ph.D. thesis and *Rep.* E-200.7. Division of Engineering and Applied Science, California Institute of Technology, Pasadena, CA.

CAMPBELL, C. S. 1986*a* The effect of microstructure development on the collisional stress tensor in a granular flow. *Acta Mech.* **63**, 61–72.

CAMPBELL, C. S. 1986*b* Computer simulation of rapid granular flows. *Proc. 10th Natl Cong. of Appl. Mech., Austin Texas, June 1986.*

CAMPBELL, C. S. 1987 Boundary interactions for two-dimensional granular flows: asymmetric stresses and couple stresses. *Proc. US-Japan Seminar on the Micromechanics of Granular Material, Sendai-Zao, Japan, October 26–30, 1987.*

CAMPBELL, C. S. & BRENNEN, C. E. 1985*a* Computer simulation of granular shear flows. *J. Fluid Mech.* **151**, 167–188.

CAMPBELL, C. S. & BRENNEN, C. E. 1985*b* Chute flows of granular material: some computer simulations. *Trans. ASME* E: *J. Appl. Mech.* **52**, 172–178.

CAMPBELL, C. S. & GONG, A. 1986 The stress tensor in a two-dimensional granular shear flow. *J. Fluid Mech.* **164**, 107–125.

CAMPBELL, C. S. & GONG, A. 1987 Boundary conditions for two-dimensional granular flows. *Proc. Sino-US Intl Symp. on Multiphase Flows, Hangzhou, China, August, 1987,* vol I, pp. 278–283.

CAMPBELL, C. S. & WANG, D. G. 1986 The effective conductivity of shearing particle flows. *Proc. 8th Intl Heat Trans. Conf.* vol. 4, pp. 2567–2572.

CHAPMAN, S. & COWLING, T. G. 1970 *The Mathematical Theory of Non-Uniform Gases*, 3rd edn. Cambridge University Press.

CUNDALL, P. A. 1974 A computer model for rock-mass behavior using interactive graphics for input and output of geometrical data. *US Army Corps. of Engrs (Missouri River Div.) Tech. Rep.* MRD-2074.

HAFF, P. K. 1983 Grain flow as a fluid mechanical phenomenon. *J. Fluid Mech.* **134**, 401–430.

HAFF, P. K. & WERNER, B. T. 1986 Computer simulation of the mechanical sorting of grains. *Powder Technol.* **48**, 239–245.

HANES, D. M. 1983 Studies on the mechanics of rapidly flowing granular-fluid materials. Ph.D. thesis, University of California, San Diego.

HANES, D. M. & INMAN, D. L. 1985 Observations of rapidly flowing granular-fluid flow. *J. Fluid Mech.* **150**, 357–380.

HEYES, D. M. 1986 The nature of extreme shear thinning in simple liquids. *Molec. Phys.* **57**, 1265–1282.

HOPKINS, M. A. 1985 Collisional stresses in a rapidly deforming granular flow. MS thesis, Clarkson University, Potsdam, NY, USA.

HOPKINS, M. A. & SHEN, H. H. 1987 A Monte Carlo simulation of a rapid simple shear flow of granular materials. *Proc. US–Japan Seminar on the Micromechanics of Granular Material, Sendai-Zao, Japan, October 26–30, 1987.*

JENKINS, J. T. & RICHMOND, M. W. 1985*a* Grad's 13-moment system for a dense gas of inelastic spheres. *Arch. Rat. Mech. Anal.* **87**, 355–377.

JENKINS, J. T. & RICHMOND, M. W. 1985*b* Kinetic theory for plane flows of a dense gas of identical, rough, inelastic, circular disks, *Phys. Fluids* **28**, 3485–3494.

JENKINS, J. T. & RICHMOND, M. W. 1986 Boundary conditions for plane flows of smooth, nearly elastic, circular disks. *J. Fluid Mech.* **171**, 53–69.

JENKINS, J. T. & SAVAGE, S. B. 1983 A theory for the rapid flow of identical, smooth, nearly elastic particles. *J. Fluid Mech.* **130**, 187–202.

KANATANI, K. 1979*a* A micropolar continuum theory of granular materials. *Intl J. Engng Sci.* **17**, 419–432.

KANATANI, K. 1979*b* A continuum theory for the flow of granular materials. In *Theoretical and Applied Mechanics* (ed. Japan Natl Comm. for Theor. and App. Mech.), vol. 27, pp. 571–578.

KANATANI, K. 1980 A continuum theory for the flow of granular materials (II), In *Theoretical and Applied Mechanics* (ed. Japan Natl Comm. for Theor. and App. Mech.), vol. 28, pp. 485–497.

LEES, A. W. & EDWARDS, S. F. 1972 The computer study of transport processes under extreme conditions. *J. Phys.* C: *Solid State Phys.* **5**, 1921–1929.

LUN, C. K. K., SAVAGE, S. B., JEFFREY, D. J. & CHEPURNIY, N. 1984 Kinetic theories for granular flow: inelastic particles in Couette flow and slightly inelastic particles in a general flow field. *J. Fluid Mech.* **140**, 223–256.

LUN, C. K. K. & SAVAGE, S. B. 1987 A simple kinetic theory for granular flow of rough, inelastic, spherical particles. *Trans. ASME* E: *J. Appl. Mech.* **63**, 47–53.

MCTIGUE, D. F. 1978 A model for stresses in shear flows of granular material. *Proc. US–Japan Seminar on Continuum-Mechanical and Statistical Approaches in the Mechanics of Granular Materials*, pp. 266–271.

NAKAGAWA, M. 1987 Kinetic theoretical approach for rapidly deforming granular material, *Proc. US–Japan Seminar on the Micromechanics of Granular Material, Sendai-Zao, Japan, October 26–30, 1987.*

OGAWA, S. & OSHIMA, N. 1977 A thermomechanical theory of soil-like materials, In *Theoretical and Applied Mechanics* (ed. Japan Natl Comm. for Theor. and App. Mech.), vol. 25, pp. 229–244.

OSHIMA, N. 1978 Continuum model of fluidized granular media. *Proc. US–Japan Seminar on Continuum Mechanical and Statistical Approaches in the Mechanics of Granular Materials*, pp. 189–202.

OSHIMA, N. 1980 Dynamics of fluidized granular material. In *Theoretical and Applied Mechanics* (ed. Japan Natl Comm. for Theor. and App. Mech.), vol. 28, pp. 475–484.

SAVAGE, S. B. 1979 Gravity flow of cohesionless granular materials in chutes and channels. *J. Fluid Mech.* **92**, 53–96.

SAVAGE, S. B. & JEFFREY, D. J. 1981 The stress tensor in a granular flow at high shear rates. *J. Fluid Mech.* **110**, 255–272.

SAVAGE, S. B. & SAYED, M. 1984 Stresses developed by dry cohesionless granular materials in an annular shear cell. *J. Fluid Mech.* **142**, 391–430.

WALTON, O. R. & BRAUN, R. L. 1986*a* Viscosity and temperature calculations for shearing assemblies of inelastic, frictional disks. *J. Rheol.* **30**, 949–980.

WALTON, O. R. & BRAUN, R. L. 1986*b* Stresses calculations for assemblies of inelastic spheres in uniform shear. *Acta Mech.* **63**, 73–86.

WERNER, B. T. & HAFF, P. K. 1985 The collisional interaction of a small number of confined, inelastic grains. *Proc. Intl Symp.-Workshop on Particulate and Multiphase Processes, 16th Annual Meeting of the Fine Particle Society, Miami Beach, Florida, USA, April 22–26.*

WERNER, B. T. & HAFF, P. K. 1986 A simulation study of the low energy ejecta resulting from single impacts in eolian saltation. *Proc. ASCE Conf.*, Minneapolis, Minnesota, USA.